Theoretical study of the field-induced pattern formation in magnetic liquids

J. Richardi,* D. Ingert,† and M. P. Pileni ‡
Laboratoire des Matériaux Mésoscopiques et Nanométriques, UMR CNRS 7070, Université Pierre et Marie Curie (Paris VI), Boîte Postale 52, 4, place Jussieu, 75230 Paris Cedex 05, France
(Received 1 March 2002; published 28 October 2002)

When a thin layer of magnetic fluid confined with an immiscible nonmagnetic liquid is subjected to a perpendicular field, the formation of hexagonal and labyrinthine patterns is observed experimentally. To develop a coherent theoretical description of this phenomenon, the free energy functionals of both types of magnetic structures are derived. Both energy functionals have the same form, which explains that the theoretical results found in this paper for hexagonal and labyrinthlike striped patterns are analogous. The size of the patterns is determined by minimizing the free energy. The influence of the method for computing the magnetic energy on the theoretical results is studied. An accurate computation of the magnetic energy proves important in predicting the experimental pattern size as a function of external field and of layer height. How the results change, when a constant magnetization is assumed during the pattern formation is also investigated. The transition between hexagonal and striped structures is studied by a comparison of their free energies. The ratio of the magnetic to the nonmagnetic liquid is found to be an important factor for the relative stability of the patterns. In agreement with experiments, striped structures are observed at large phase ratios, whereas at small phase ratios hexagonal patterns predominate.

DOI: 10.1103/PhysRevE.66.046306 PACS number(s): 47.54.+r, 47.65.+a, 77.84.Nh

I. INTRODUCTION

When magnetic fluid films are subjected to an external magnetic field, the formation of static patterns can be observed experimentally [1]. For a field perpendicular to the plane of the film, two types of patterns are found: labyrinths and hexagonal arrays of columns. The formation of labyrinths was reported in Refs. [2–5] (labyrinthine instability), where the magnetic fluid is confined with an immiscible nonmagnetic liquid between closely spaced horizontal glass plates (Hele-Shaw cell). Labyrinths were also observed in thin layers of demixed ferrofluids [6] or of magnetic liquids forming aggregates [7] sealed in a Hele-Shaw cell with a height of several micrometers. A variation of the field strength can lead to a transition between labyrinthine and hexagonal structures [5–8]. Hexagonal patterns also appear at the free surface of magnetic fluids subjected to a vertically oriented magnetic field (Rosensweig instability) [1]. In our laboratory, solid mesostructures of cobalt nanocrystals were recently observed, when a solution of the magnetic nanoparticles is evaporated while applying a magnetic field [9]. These mesostructures are also of hexagonal and labyrinthine types.

The patterns are formed by the interface between the magnetic and the nonmagnetic phases and their formation can be explained by the competition between the magnetic and the surface energy. The surface tension tends to minimize the area of the interface, whereas the interaction between the magnetic dipoles favors an extended interface.

An understanding of the formation of these patterns is of general interest. In a wide variety of physical and chemical systems, the formation of similar structures is also attributed to the presence of competing interactions. Thus, labyrinths and hexagonal patterns appear in magnetic garnets, amphiphilic ''Langmuir'' layers, films of block copolymers and type I superconductors subjected to magnetic fields [10–13].

A theoretical approach to describe the pattern formation in ferrofluids is proposed. The results obtained by this method (called *''A''*) are compared to those of two approaches (called *''B''* and *''C''*), which were proposed in the literature [4,14]. All three methods are based upon a minimization of the free energy which was already successfully used to study the Rosensweig instability [15,16]. The main difference between the three methods is the way of computing the magnetic energy, for which an exact computation is still a complicated task. In method *A*, the magnetic energy is calculated in the most accurate way. In particular, the *nonuniformity* of the demagnetization field is taken into account. Usually, the energy difference between hexagonal and striped patterns is very small as we will show in the following. Therefore, high accuracy in the energy calculation is especially important in the study of the transition between both structures, which is one of our objectives. The less accurate method *B* was proposed by Rosensweig *et al.* [4] who developed a theory for spacing of the labyrinthine stripes. The approximation was made that the demagnetization field is *uniform* and equal to that in the center of the labyrinthine stripes. It was recently shown that this approach predicts the size and spacing of the stripes in good agreement with experiments only at low fields [17]. At high fields, method *B* fails to predict the decrease in the stripe width, which is correctly reproduced by method *A*. A third way of computing the magnetic energy (method *C*) was recently used by Ytreberg and McKay [14], who developed a theory to predict the size and spacing of aggregates in a hexagonal pattern as a function of the external field and the cell height. Their approach is based upon the

*Electronic address: richardi@sri.jussieu.fr
†Electronic address: ingert@sri.jussieu.fr
‡Author to whom correspondence should be addressed; electronic address: pileni@sri.jussieu.fr; URL: http://www.sri.jussieu.fr

assumption of a *constant* magnetization during the pattern formation due to particle aggregation.

A minimization of the free energy containing surface, magnetic, and entropy terms gives the most favorable size and energy of the patterns.

The objective of this paper is twofold. First, the influence of the methods *A*, *B*, and *C* of computing the magnetic energy upon the theoretical results is studied. The theoretical predictions are compared to experimental data. Second, the energy functionals are derived for striped and hexagonal patterns. This enables us to compare the geometry and energy of both types of ferrofluid patterns. Thus, the relative stability of structures and possible transitions between labyrinthine and hexagonal patterns can be investigated theoretically. To our knowledge, the theories published in the literature have been restricted to either labyrinthine [4,17] or hexagonal patterns [14] except for a very recent mean-field approach [18]. As the energies of both types of patterns are usually very close (less than 2%), the free energy must be evaluated with a high numerical precision to give correct information on the relative stability.

The labyrinth is described by an idealized pattern of parallel stripes. The presence of convolutions and nodes in real labyrinth are likely the result of nonequilibrium growth. These features are neglected in our approach following Rosensweig *et al.* [4,17].

The paper is organized as follows. In Sec. II, the free energy functional for striped and hexagonal patterns are derived and the different ways of computing the magnetic energy are discussed. In Sec. III, we describe the properties of the ferrofluid systems, which are investigated here. The theoretical and experimental trends as a function of the field strength and of the cell height are compared in Sec. IV. Finally, the transition between hexagonal and striped patterns is investigated. These results are compared to experiments and other theories.

II. THEORY

A. Description of the magnetic patterns

Following Rosensweig *et al.* [1,4], the labyrinth is idealized as a repeating pattern of infinitely long parallel stripes. The hexagonal pattern is described as a hexagonal array of cylindrically-shaped magnetic matter (see, Fig. 1). Recent experiments [19] have shown that aggregates in ferrofluids emulsions can have tapered or split ends. Here, we will restrict ourselves to the study of idealized structures, because the theoretical results obtained using this approach are in good agreement with experimental data [17]. Drikis *et al.* [20] recently studied the formation of real labyrinthine patterns by a theoretical approach. They show that the stripe-stripe distances of realistic labyrinthine patterns agree well with the values calculated for the idealized system of straight stripes studied here. Therefore, we think that in spite of the strong idealization the used description of the structures can give reasonable estimates of the pattern size. Moreover, the inherent symmetries of these patterns can be used to compute very precise estimates of the free energy.

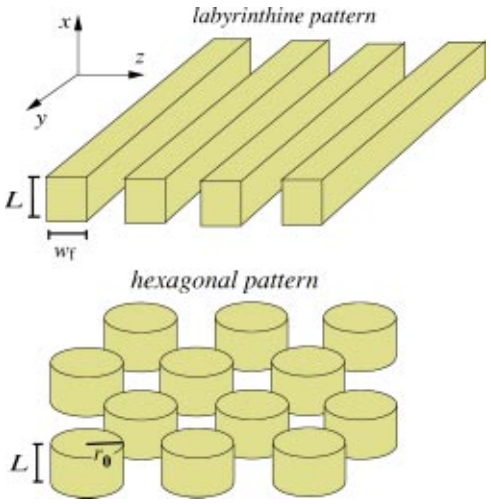

FIG. 1. Sketch of the idealized structures used to describe labyrinth and hexagonal patterns. The shown structural fragments repeat themselves to form an infinite periodic pattern in the *y* and *z* directions. The geometric parameters are illustrated and the used global frame is shown.

The nomenclature is illustrated in Fig. 1. L denotes the height of the cell. For the hexagonal pattern, the radius of a cylinder is r_0, while the width of a labyrinthine stripe is denoted by w_f. The energetically most favorable value of r_0 or w_f depends on the external field H_0, the pattern height L, the magnetic susceptibility χ, the interfacial tension σ and the volume fraction ϕ of the magnetic fluid. In the selected laboratory frame, the x axis is parallel to the direction of the external magnetic field and for the striped pattern, the stripes are along the y axis.

B. Magnetic energy

The free energy of the hexagonal and striped patterns will be formulated as the sum of the magnetostatic term F_m, the surface term F_s and the entropy term $-TS$. In the following section the computation of the magnetic energy is explained for the most accurate approach *A*. Then, it will be shown how the calculations change when the approximations of methods *B* and *C* are introduced.

Method A. According to classical magnetostatics (see, Jackson [21], page 213) the energy change resulting from the introduction of a magnetic medium to an empty region can be written as

$$F_m=\frac{1}{2}\int \mathbf{H}\cdot\mathbf{B}d\mathbf{r}-\frac{\mu_0}{2}\int \mathbf{H}_0^2 d\mathbf{r} \tag{1}$$

$$=-\frac{\mu_0}{2}\int_{V_m}\mathbf{M}(\mathbf{r})\cdot\mathbf{H}_0 d\mathbf{r}. \tag{2}$$

V_m indicates that the integral is over the volume of the magnetic medium. The magnetic induction $\mathbf{B}$ is given by the relationship $\mathbf{B}=\mu_0(\mathbf{H}+\mathbf{M})$. The total magnetic field $\mathbf{H}(\mathbf{r})$ at a point $\mathbf{r}$ within a stripe or a cylinder is the intensity of the applied field $\mathbf{H}_0$ less the demagnetization field $\mathbf{H}_d(\mathbf{r})$,

$$\mathbf{H}(\mathbf{r}) = \mathbf{H}_0 + \mathbf{H}_d(\mathbf{r}). \tag{3}$$

Equation (1) only holds for magnetic media with a linear relationship between the magnetization $\mathbf{M}(\mathbf{r})$ and the magnetic field $\mathbf{H}(\mathbf{r})$:

$$\mathbf{M}(\mathbf{r}) = \chi \mathbf{H}(\mathbf{r}) = \chi[\mathbf{H}_0 + \mathbf{H}_d(\mathbf{r})], \tag{4}$$

where Eq. (3) was used. χ is the susceptibility of the medium within the cylinders or stripes.

The demagnetization field $\mathbf{H}_d(\mathbf{r})$ is calculated as follows. First, the field $\mathbf{H}_i(\mathbf{r}_i)$ due to a single cylinder or stripe with its center at $\mathbf{r}_i$ is evaluated from (see, Jackson [21], p. 186)

$$\mathbf{H}_i(\mathbf{r}_i) = \int_{V_m} d\mathbf{r}\, \frac{1}{4\pi(\mathbf{r}-\mathbf{r}_i)^3} \times \left\{ -\mathbf{M}(\mathbf{r}) + \frac{3[\mathbf{M}(\mathbf{r})\cdot(\mathbf{r}-\mathbf{r}_i)](\mathbf{r}-\mathbf{r}_i)}{(\mathbf{r}-\mathbf{r}_i)^2} \right\}. \tag{5}$$

Due to the complex dependence of $\mathbf{M}(\mathbf{r})$ upon $\mathbf{r}$, the integrals cannot be solved analytically. Therefore, the integrals were evaluated making use of the Romberg method [22]. To reduce the computing time, the variation of $\mathbf{M}(\mathbf{r})$ in the x direction was neglected during the evaluation of $\mathbf{H}_i(\mathbf{r})$. Therefore, the magnetization $\mathbf{M}(\mathbf{r})$ can be replaced by its x-averaged value $\overline{\mathbf{M}}(\mathbf{r})$ in Eq. (5).

The $\mathbf{H}_i$ values of all cylinders or stripes are summed up to obtain the total demagnetization field at $\mathbf{r}$:

$$\mathbf{H}_d(\mathbf{r}) = \sum_i \mathbf{H}_i(\mathbf{r}-\mathbf{r}_i), \tag{6}$$

where $\mathbf{r}_i$ are the center positions of the labyrinthine stripes or of the cylinders in a hexagonal grid.

The details of the calculation of the demagnetization field are explained in the Appendix. In particular, the correct treatment of the long-range dipolar interactions is derived.

The magnetization in a hexagonal pattern is obtained by an iterative procedure for a given set of parameters ϕ, χ, H_0, L, and r_0. It starts with the choice of an arbitrary initial magnetization $\mathbf{M}_{\text{guess}}(\mathbf{r})$. Then, at a large number of points in the cylinder, the demagnetization field is calculated from the magnetization using Eqs. (A2) and (6). The long-range correction from Eq. (A4) is taken into account. At each point a new estimate of the magnetization is calculated from

$$M_{x,\text{new}}(\mathbf{r}) = \frac{\chi H_0}{1 - \chi H_{d,x}(\mathbf{r})/\overline{M}_{x,\text{guess}}(\mathbf{r})}. \tag{7}$$

The use of this equation instead of the analogous relationship (4) greatly speeds up the convergence of the iterative procedure.

Self-consistency is reached, if the new magnetization $\mathbf{M}_{\text{new}}(\mathbf{r})$ agrees with $\mathbf{M}_{\text{guess}}(\mathbf{r})$. If self-consistency is not reached, the iterative procedure restarts with the calculation of the demagnetization field for the new magnetization as $\mathbf{M}_{\text{guess}}(\mathbf{r})$. For the striped pattern, the magnetization is obtained by an analogous iterative procedure.

Method B. This approach is the corrected form [17] of the theory proposed by Rosensweig *et al.* [1]. The magnetic energy is obtained from the magnetization using Eq. (2) as before. The only difference from method *A* is the assumption of a uniform demagnetization field in the pattern. The demagnetization fields $\mathbf{H}_d(\mathbf{0})$ at the center of the cylinders or stripes are calculated as before using an arbitrary uniform magnetization M'. Then the magnetization is approximated by $M_x(\mathbf{r}) \approx \chi H_0/(1-\chi H_{d,x}(\mathbf{0})/M')$ [see, Eq. (7)]. An iteration as in method *A* is not necessary.

Method C. This method is based on the assumption introduced by Cebers and Maiorov [3] and used in many papers [14,20,23–25] that the magnetization of the ferrofluid is constant during the formation of patterns. This is a reasonable assumption for patterns which form due to the aggregation of ferromagnetic particles coated by surfactant with long alkyl chains [26]. Hong *et al.* [7] show that the particles form small chains immediately after the application of the field. Then, during the rather slow pattern formation, the particles cannot change their orientation due to the interdigitation of the alkyl chains. If the particles are not superparamagnetic, the magnetic dipoles of the particles do not change during the pattern formation due to the fixed orientations. This leads to a constant magnetization within the aggregates during the pattern formation. The magnetization is uniform and has the value observed before the pattern formation. Due to the constant magnetization, the magnetic induction $\mathbf{B}$ in Eq. (1) must be replaced by the magnetic field $\mathbf{H}$:

$$F_m = \frac{\mu_0}{2}\int \mathbf{H}\cdot\mathbf{H} d\mathbf{r} - \frac{\mu_0}{2}\int \mathbf{H}_0^2 d\mathbf{r} = \mu_0 \int \mathbf{H}_d\cdot\mathbf{H}_0 d\mathbf{r} + \frac{\mu_0}{2}\int \mathbf{H}_d\cdot\mathbf{H}_d d\mathbf{r}, \tag{8}$$

where Eq. (3) was used.

The first term on the right side does not change during the pattern formation and can be ignored in the energy minimization. The second term represents the repulsion of the magnetic dipoles induced by the external field. The dipoles can be represented as monopoles at the ends of the cylinders or stripes with the charge $\mu_0 M dz dy$. Therefore, the second term of F_m can be also calculated from the interaction between the magnetic monopoles [see, Rosensweig [1], page 30]:

$$F_{m,2} = \sum_{i=1}^{N_0} \frac{M^2\mu_0}{4\pi}\int dy_1 dz_1 \int dy_i dz_i \times \left\{ \frac{1}{\sqrt{(\mathbf{s}_1-\mathbf{s}_i)^2}} - \frac{1}{\sqrt{(\mathbf{s}_1-\mathbf{s}_i)^2 + L^2}} \right\}. \tag{9}$$

The sum is over all cylinders or stripes in the pattern. The first term in the parenthesis is the repulsion between the tops and between the bottoms. The second term is the attraction between the ends in opposite planes. $\mathbf{s}_i = (y_i, z_i)$ denotes all

points at the top of the cylinder or stripe *i*. Long-range corrections are calculated in a way analogous to that which will be shown for the demagnetization field in the Appendix.

Jackson *et al.* [24] show that there are two other equivalent forms of computing the magnetic energy beside Eq. (9). In particular, the third form derived in Ref. [24] is useful in the computation for realistic models of labyrinthine patterns. For the idealized structures studied here the integrals in Eq. (9) were solved analytically and it was not necessary to use the other forms proposed in Ref. [24].

In method *C* the magnetization is calculated from its initial value $\mathbf{M}_{\text{init}}$ observed before the pattern formation:

$$\mathbf{M}=\frac{\mathbf{M}_{\text{init}}}{\phi}=\frac{\chi_{\text{init}}\mathbf{H}_{\text{init}}}{\phi}, \tag{10}$$

where $\chi_{\text{init}}=\phi\chi$ is the initial susceptibility, $\mathbf{H}_{\text{init}}=\mathbf{H}_0+\mathbf{H}_{d,\text{init}}$ and $\mathbf{H}_{d,\text{init}}=-\mathbf{M}_{\text{init}}$. The way of calculating the magnetization differs from that used in other papers [20,23–25].

Comparison of the three methods

To sum up, there are three different approaches to compute the magnetic energy. In approaches *A* and *B*, F_m is obtained from the magnetization using Eq. (2). It is assumed that the magnetization changes during the pattern formation. In the first approach, *A*, the magnetization is calculated by a self-consistent iterative procedure which has been discussed above. The only approximation is the neglect of the variation of the magnetization in the *x* direction. Preliminary results show that the deviation of the magnetic energy caused by this approximation is less than 1% [27]. This should be compared to the energy difference of about 5% caused by the approximations of method *B* proposed by Rosensweig *et al.* [4]. This approach assumes a uniform demagnetization field. The magnetization is calculated from its value at the center of the cylinders or stripes. The third approach *C* consists of the use of Eq. (9) implying a constant magnetization during the pattern formation. Of course, the value of the magnetic energy obtained by this method is completely different from the results of approaches *A* and *B*.

C. Surface energy and entropy term

Several forms of the surface energy have been used in the literature. For electrorheological fluids, Halsey and Torr [28] propose a surface term, that depends upon the electric field. The same form was also used by Liu *et al.* [29] for magnetorheological fluids. The dependence of the surface term on the field accounts for the differences between the local fields experienced by the nanoparticles at the surface and inside the cylinders or stripes. In contrast to Liu *et al.* [29] we explicitly take the nonuniformity of the demagnetization field into account except for method *B*. Therefore, we will use a simple hypothesis introduced by Rosensweig *et al.* [4], which assumes that the interfacial tension σ is independent of the field and depends only on the two substances present at the interface. Measurements of ferrofluid surface tensions in confined geometries support this hypothesis [30]. Since we assumed a cylindrical shape of the magnetic matter, we must introduce two terms for the surface energy of the hexagonal pattern: one for the sides and the other one for the top and for the bottom. The surface energy for a single aggregate is then

$$F_{s,h}=\sigma(2\pi r_0 L)+2\sigma'(\pi r_0^2), \tag{11}$$

where σ and σ' denote the interfacial tension at the sides and at the ends of the cylinders, respectively.

In order to compare the surface energy of the hexagonal patterns for different radii r_0, $F_{s,h}$ is divided by the average surface area per cylinder s_h,

$$s_h=\pi r_0^2/\phi. \tag{12}$$

Only the first term of the resulting equation depends on r_0. Therefore, the second term can be ignored when the energetically favored radius of the cylinders is calculated (compare with Ref. [14]).

The surface energy of a stripe in a labyrinth is given by [4]

$$F_{s,l}=2\sigma(y_0 L)+2\sigma'(y_0 w_f), \tag{13}$$

where y_0 is the length of the stripe. F_s is divided by the average surface area per stripe

$$s_l=y_0 w_f/\phi. \tag{14}$$

For the same reason as discussed above the second term of Eq. (13) can be ignored.

For micrometric cell heights, the entropy term of the free energy is expected to become significant. Therefore, Ytreberg and McKay [14], calculated the entropy from the number N_0 of aggregates in the cell. They proposed to use $N_0!$ for the number of states accessible to the system. Using the entropy term $k_B T \ln N_0!$ we have found that it is only important in determining the pattern geometry at values for *L* smaller than 2 μm. As we restrict our study to cell heights larger than 2 μm, this entropy term is not taken into account in the following. Moreover, we are not sure that the equation $N_0!$ gives the correct number of accessible states. To our mind, this approach neglects the fact that the number of particles in the aggregates changes with N_0. Another form of taking the entropy into account is the use of the entropy of a gas on a lattice [18]. But in our way of describing the patterns this term is zero. More sophisticated entropy models are now being developed and might prove of interest in future studies of pattern formation on mesoscopic scales [9].

D. The free energy functional of patterns in ferrofluids

In the methods *A* and *B* the free energy per surface area for the hexagonal pattern is formed by combining Eqs. (2), (11), and (12). When we eliminate the terms which do not depend on r_0 we arrive at

$$F_h=\phi\left\{2\frac{L}{r_0}\sigma-\frac{1}{2}\mu_0 L\langle M\rangle_h H_0\right\}, \tag{15}$$

where $\langle M\rangle_h$ is the volume-averaged magnetization in the magnetic phase of the hexagonal pattern.

Using Eqs. (2), (13), and (14) the free energy functional for the striped pattern can be written as

$$F_l=\phi\left\{2\frac{L}{w_f}\sigma-\frac{1}{2}\mu_0 L\langle M\rangle_l H_0\right\}. \tag{16}$$

$\langle M\rangle_l$ is the volume-averaged magnetization in the magnetic phase of the stripes. In method *C*, the magnetic energy term is replaced by the expression in Eq. (9).

In accordance with Refs. [1,4,14,29] we treat the pattern formation as a quasiequilibrium process. Indeed, studies on the dynamics of labyrinth formation indicate that the final geometry of the patterns is largely determined by the structure of the energy functional [23]. Thus, reasonable estimates of the sizes r_0 and w_f can be obtained by a minimization of the free energy given in Eqs. (15) and (16), respectively. The minima are located numerically using the Newton-Raphson method [22].

Let us compare Eqs. (15) and (16). We find that the free energy functional has the same form for a hexagonal and a striped pattern except for an exchange of r_0 and w_f. Moreover, we will show that the field and, therefore, the magnetization are very similar in both structures for the same values of r_0 and w_f. The similarity of the energy functionals explains why the theoretical trends observed for hexagonal and striped patterns are analogous, as will be shown in Sec. IV.

III. STUDIED SYSTEMS

The pattern formation in very different systems can be studied using the theory proposed here. Systems range in diversity from ferrofluids confined with immiscible liquids [4,5] to magnetic liquids forming aggregates [7,29]. To arrive at general conclusions on the field-induced pattern formation, we have chosen to study two completely different systems.

(i) System 1 was examined both theoretically and experimentally by Rosensweig *et al.* [4]. A ferrofluid is confined with an immiscible nonmagnetic fluid between two parallel plates separated by a height varying from 0.4 to 1.2 mm. The experimental values of the initial susceptibility and the interfacial tension are taken from Ref. [4] ($\chi=1.6$ and $\sigma=0.0043$ Nm^{-1}).

(ii) System 2 is a pure ferrofluid confined between two plates with a separation of several micrometers as studied in the experiments of Ref. [7] . The application of the magnetic field causes a separation of the ferrofluid into a highly concentrated and a very diluted magnetic phase. The hexagonal and labyrinthine patterns are made of the concentrated phase, where the magnetic particles can form aggregates and, therefore, method *C* can give valuable information. In comparison with system 1, the second one is characterized by a larger susceptibility and a much smaller interfacial tension. In accordance with Ref. [14], we assume that the magnetic particles are randomly packed in the cylinders or stripes. Then, the volume fraction of magnetic particles in the aggregates is equal to the packing fraction for randomly placed spheres ($\gamma=0.638$). The magnetic particles studied experimentally in Ref. [7] have an average diameter *d* of 11.8 nm. From the particle diameter *d*, the volume fraction γ and the domain magnetization of magnetite (4.46×10^5 Am^{-1}) the initial susceptibility within the aggregates can be estimated from the Langevin formula [Ref. [1], page 59]. A value of 11.7 for χ is found. We employ the interfacial tension proposed by Ytreberg and Mckay [14] in their study of the experiments by Hong *et al.* ($\sigma=1.1\times10^{-6}$ Nm^{-1}). The small value of σ is in accordance with Bacri *et al.* [6], who find for their systems of demixed ferrofluids, that the surface tension between the two co-existent demixed phases is 10 000 times lower than in ordinary liquids.

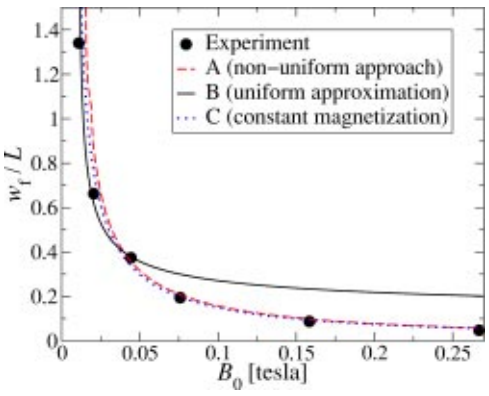

FIG. 2. Dependence of the normalized stripe width w_f/L in labyrinths on the external field H_0 for system 1. The theoretical results of the three methods of computing the magnetic energy are compared to experimental data. The cell height and volume fraction are fixed at $L=0.9$ mm and at $\phi=0.5$. The experimental points were obtained from Ref. [4].

A systematic study for both systems using ϕ values between 0.1 and 0.8 has been carried out. System 1 is studied at field intensities up to 0.25 T and for heights between 0.4 mm and 1.2 mm in accordance with the experimental results given by Rosensweig *et al.* [4]. For system 2, the height *L* varies from 1 μm to 50 μm. The highest field strengths studied for this system range up to 0.03 T. At each state point, the aggregate size is found by minimization of the free energy using the three different methods for the calculation of the magnetic energy discussed above. We want to emphasize that the results presented in the following section for particular states are used to illustrate the general conclusions drawn from the systematic study.

IV. RESULTS

A. Dependence of the results on the theoretical approach

In this section, we first compare the pattern sizes predicted by the three different methods of computing the magnetic energy. The evolution of the pattern size is studied as a function of the field strength and of the cell height. Here, we focus on either striped or hexagonal structures. The transition between both structures is studied in the following section.

In Fig. 2, plots of the energetically favorable width of the labyrinthine stripes as a function of H_0 are shown for the

three approaches. The χ and σ values correspond to system 1. The volume fraction and the cell height are fixed at $\phi = 0.5$ and at $L = 0.9$ mm. These parameters were chosen, because experimental data were published for this system in Ref. [4]. The dots in Fig. 2 are the experimental data points obtained from Ref. [4]. Rosensweig *et al.* [4] found that approach *B* correctly predicts the experimental data in the whole range of studied fields. Recently, we observed that this good agreement between theory and experiment at high fields was only due to errors in the computation of the theoretical values made in Ref. [4] (see, discussion in Ref. [17]). A correct recalculation of the energetically favorable stripe widths using approach *B* indicates excellent agreement with the experimental data at low fields, as can be seen in Fig. 2. In contrast, approach *B* is not able to correctly reproduce the decrease in w_f on increasing the field. The small variation of w_f at high fields is due to the fact that the homogeneous limit of the magnetic energy expected for $w_f \to 0$ is already reached for values of $w_f/L \approx 0.3$ [17]. Therefore, a further reduction of the stripe width does not change the magnetic energy and cannot contribute to a minimization of the free energy.

The comparison with the results obtained from method *A* using a nonuniform demagnetization field shows the influence of the uniform approximation of approach *B* on the calculated stripe widths. In both methods a minimum field value of about 0.01 T is required to establish the striped pattern. The approach using nonuniform magnetization predicts a larger threshold value of H_0 for the pattern formation. This larger threshold value cannot be confirmed by experiments. At low fields the new approach *A* gives larger stripe widths. The decay of the stripe width observed experimentally can be correctly reproduced by method *A*. Obviously, the neglect of the nonuniformity of the magnetization in method *B* is an important factor, causing the wrong behavior of the approach proposed by Rosensweig *et al.* [4] at high fields.

Methods *A* and *C* give very close results. This is somewhat surprising, because the two methods explain the pattern formation in very different ways. In method *A*, the pattern formation leads to a less negative demagnetization field. Since $\mathbf{M} = \chi(\mathbf{H}_0 + \mathbf{H}_d)$, the magnetization within the ferrofluid increases and, according to Eq. (2), the magnetic energy is reduced with formation of striped or hexagonal patterns. In approach *C*, assuming a constant magnetization, the pattern formation is explained by the reduction of the interaction energy between the magnetic moments caused by the intercalation of a nonmagnetic phase within the magnetic matter. We conclude that the assumption of a constant magnetization does not necessarily lead to a different size of the pattern, which could be easily distinguished experimentally.

We now turn to the variation of the pattern size with the cell height. Figure 3 is a plot of the energetically favorable radius of cylinders as a function of the height *L* using the three methods to compute the magnetic energy. The values of χ and σ correspond to system 2. The external field and the volume fraction are fixed at $B_0 = 0.005$ T and at $\phi = 0.5$, respectively. In comparison with method *B*, the results for constant (method *C*) and nonuniform magnetization (method *A*) are close. The results of the micrometric system 2 are shown here, because most of the experimental studies on the decrease of the pattern size with the height were carried out under similar conditions [7,9,29,31]. Except at very small *L*, our theoretical data points can be well represented by a power law of the form $r_0 = \alpha L^{\beta}$. For methods *A* and *C*, we find an exponent close to 0.5, whereas approach *B* yields a very different exponent around 0.9. These values can be compared with those obtained by a fit to experimental data in the literature. In Ref. [31] the exponent varies between 0.5 and 0.67. Liu *et al.* [29] obtained an exponent of 0.37 for experiments with magnetorheological fluids. Obviously, the exponents observed assuming nonuniform or constant magnetization fits well in the range of values observed experimentally in contrast to that of method *B*.

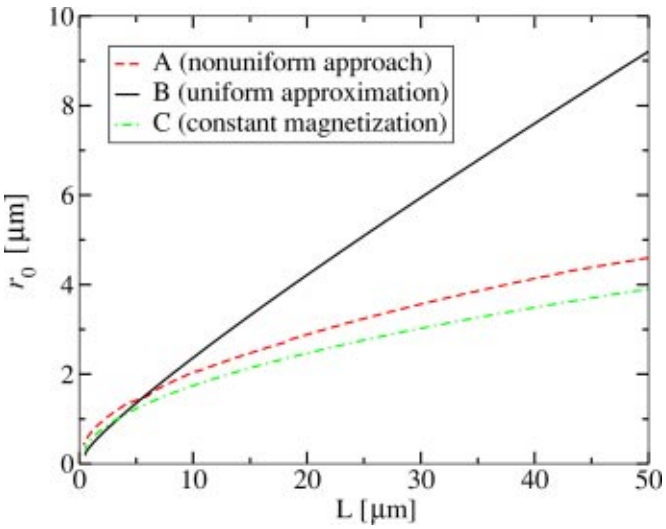

FIG. 3. Dependence of the cylinder radius r_0 in hexagonal patterns on the cell height *L* for system 2. The theoretical results of the three methods of computing the magnetic energy are compared. The external magnetic field and volume fraction are fixed at $B_0 = 0.005$ T and at $\phi = 0.5$.

B. Transitions between hexagonal and striped patterns

In several Refs. [5–7,9], the transition between hexagonal and striped structures have been observed experimentally on changing the external field or the height. But it is still not obvious, which geometric parameter should be taken to compare both patterns. We will first address to this question. Then, the transition between both patterns is studied by a comparison of their free energy.

Hong *et al.* [7] focused on the aggregate-aggregate distance to compare hexagonal and striped patterns, while Legrand *et al.* [9] used the diameters of the columns and the widths of the stripes. Figure 4 shows plots of w_f and r_0 of striped and hexagonal patterns for system 1 as a function of H_0. The results from methods *A* and *C* are shown. Method *B* gives similar agreement between w_f and r_0. The height and the volume fraction are fixed at $L = 1.0$ mm and at $\phi = 0.5$. Approaches *A* and *C* predict that under the same conditions, such as the external field, the width of the wall in a striped pattern should be close to the cylinder radius in a hexagonal

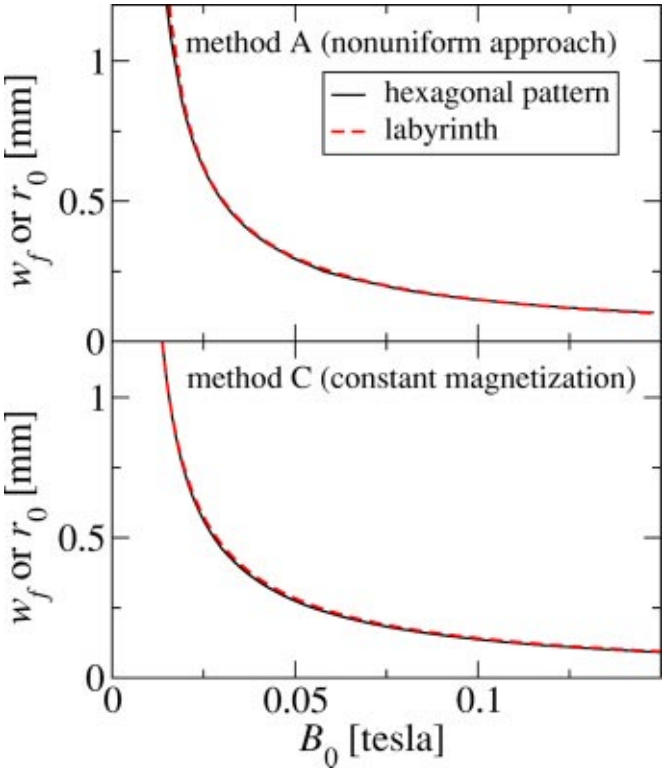

FIG. 4. Comparison of the geometrical parameters used to describe hexagonal and striped patterns. The dependences of r_0 and w_f on the external field H_0 are shown for system 1. The cell height and volume fraction are fixed at $L=1.0$ mm and at $\phi=0.5$. The results of two methods of computing the magnetic energy are plotted.

pattern. This can be explained as follows. First, as discussed in Sec. IV, the free energy functional has the same form for both patterns, when the geometries are described by w_f and r_0. Second, the demagnetization field and the magnetization are very similar in both structures for the same value for w_f and r_0. We conclude that the stripe width should be compared to the cylinder radius when striped-hexagonal transitions in ferrofluids are investigated.

Finally, a last question arises: Can we understand the transitions between hexagonal and labyrinthine structures observed experimentally [5–7,9]? Thus, the energies of both types of patterns are compared. The free energy per surface F_h and F_l of both patterns are calculated from Eqs. (15) and (16) using the energetically favorable values of r_0 and w_f. Most structural transitions are experimentally observed by a variation of the magnetic field. Therefore, the normalized energy difference $(F_l-F_h)/F_l$ in % is plotted as a function of external field. The three Figs. 5(a)–5(c) show the theoretical results for the three different ways of computing the magnetic energy. Volume fractions varying from $\phi=0.1$ to $\phi=0.8$ were studied and the results for four representative ϕ values are given. The values of χ and σ correspond to system 1. The cell height is fixed at $L=1$ mm. $(F_l-F_h)/F_l<0$ indicate a higher stability of the striped patterns, whereas $(F_l-F_h)/F_l>0$ reveals the energetical preference of hexagonal structures. All three approaches predict the existence

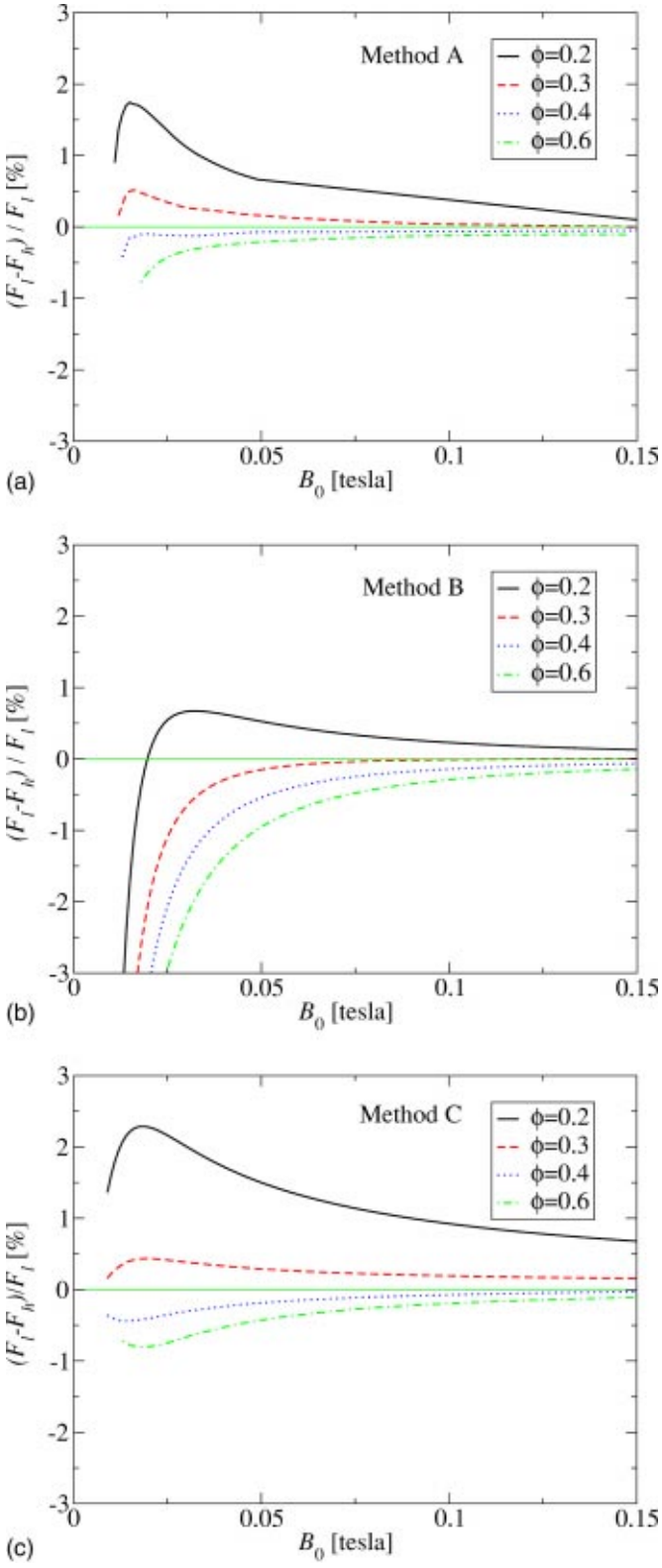

FIG. 5. Normalized free energy differences $(F_l-F_h)/F_l$ as a function of the field for four representative ratios ϕ of the magnetic to nonmagnetic phases. The results for (a) methods *A*, (b) *B*, and (c) *C* are shown for system 1. The cell height is fixed at $L=1.0$ mm.

of hexagonal patterns at low volume fractions, whereas labyrinths should predominate at large values of ϕ. For methods *A* and *C*, a critical phase ratio between $\phi=0.3$ and 0.4 is observed for the transition. The less accurate approach *B* yields a smaller transition value of ϕ. Method *B* also predicts a transition to a labyrinth at very weak fields for small ϕ, which is not confirmed by the more accurate approach *A*. The comparison of the energy differences obtained by methods *A* and *B* indicates that the consideration of the nonuniformity of the demagnetization field strongly decreases the absolute energy differences at large values of ϕ. A thorough study of the energy differences for system 2 using $L=2$ μm qualitatively led to the same conclusions. In particular, the same ϕ is found for the structural transition.

The theoretical results for the pattern stability can be compared with experiments and other theories. Our approach predicts very small energy differences, less than 1%, over a broad range of ϕ and H_0. Obviously, the morphologically very different striped and hexagonal structures can be energetically quite close. This gives the possibility of a transition between both patterns observed experimentally. The theoretical results have revealed the importance of the phase ratio for the pattern stability. A systematic experimental study of the predominant pattern as a function of ϕ is still missing. However, it is interesting that all the experiments which show the existence of hexagonal patterns were carried out at low ϕ [e.g., $\phi=0.2$ in Ref. [5] and $\phi=0.2$–0.3 in Ref. [7]]. In both experimental studies, increasing the field H_0 leads to the transition to a striped pattern. In our calculations using the accurate methods, *A* and *C*, we have never observed a transition between hexagonal and striped structures by a variation of the field. Figures 5(a)–5(c) only show that the stability of the hexagonal pattern with respect to the striped one decreases on increasing the field for small ϕ. Ytreberg *et al.* [14] proposed a theory to explain the transition between hexagonal and striped structures by a variation of the field. They observed the loss of the local minimum in the free energy of hexagonal patterns for very small and high field intensities. The loss of this minimum also appears at very small cell heights. They concluded that, in these regions of parameter space, hexagonal patterns will not be found, and a transition to other patterns could be expected. Thus, they established a phase diagram, which seems to predict the transition between hexagonal and striped patterns as a function of the magnetic field and of the cell height. In our calculations, a loss of the local minimum in F_h is also found at small H_0 (see, Fig. 2). But it is due to the fact that a minimum field strength is required to establish the pattern to counteract the interfacial tension. The same is also observed for the striped structures. Using methods *A* and *C*, we find that the theoretical threshold values of the field for the formation of hexagonal and striped patterns are almost the same. Our calculations do not predict any range of fields where only one of both patterns exists. Therefore, we cannot show that the loss of the minimum at small fields really involves a transition between hexagonal and striped structures. For all three approaches, we never observed a loss of the local minimum at high fields even with the entropy term proposed in Ref. [14]. In method *C*, which is very close to the approach in Ref. [14], the energetically favorable radius of the cylinders markedly decreases at large fields, but it is always well defined. Ng and Vanderbilt [32] studied similar transition between striped and hexagonal droplet phases in a two-dimensional (2D) model with dipolar interaction. In spite of the idealization of a two-dimensional model their results agree well with our observations. The striped structure is stable near area fraction 0.5 with transition to the hexagonal pattern at 0.286.

At the time of writing, we became aware of a mean-field approach which was developed by Lacoste and Lubensky [18] to study the pattern formation in ferrofluids. In good agreement with our results, they observe hexagonal structures at low ϕ and labyrinths at large ϕ. At an even larger phase ratio an inverted hexagonal structure is found, which was not taken into account here. In a narrow range of ϕ values they predict a field induced transition from hexagonal to striped structures. This might be due to the inclusion of entropy terms in their model, their description of the patterns using 2D Fourier transforms or the density variations allowed in their model. Recent experiments by Hong *et al.* [8] show that the transition from hexagonal to labyrinthine patterns experimentally observed in Ref. [7] must be attributed to the existence of long-range grain boundaries. If the number of grain boundaries is reduced, the field-induced transition to labyrinths is no longer observed. Obviously, experiments and theoretical studies indicate that the labyrinthine patterns experimentally observed for small volume fractions are only metastable. In fact, the theoretical study of the labyrinthine pattern formation by Langer *et al.* [23] agrees with this conclusion. They studied the evolution of a circular ferrofluid drop between two plates after applying a field. Calculations show that the modes to a fission of connected structures into smaller droplet are not the most unstable ones. Indeed, Langer *et al.* [23] observe that the initial drops always form simply connected striped pattern and never break up into smaller droplets, although the global minimum is actually obtained for widely dispersed droplets. This underscores the necessity of considering the dynamics rather than statics in understanding the kind of patterns experimentally observed.

V. CONCLUSIONS

A free energy approach was developed which predicts the experimental geometries of field-induced hexagonal and labyrinthine patterns. Correct handling of the nonuniformity of the demagnetization field is important to reproduce the experimental behavior at large fields. The experimental trends of the pattern size as a function of cell height are also better described by the nonuniform approach. Although the calculation of the magnetic energy by the method *C* is very different from the more accurate method *A*, the calculated results are quite similar. This shows that method *C* widely used in the literature [14,20,23–25] can give reliable results, in particular at high fields where method *B* fails. In spite of a completely different morphology, the theoretical results for the hexagonal and striped patterns are very close, as observed in experiments [5]. This is due to the fact that the free

energy functionals of both patterns have the same form. Under the same conditions the cylinder radius of a hexagonal pattern and the stripe width are very close. The comparison of the free energies of hexagonal and striped patterns shows the importance of the ratio of the magnetic to the nonmagnetic phases for the pattern stability. In agreement with experiments and other theories, hexagonal patterns are found at low ϕ, whereas labyrinths predominate at $\phi > 0.3$. The theory does not predict a transition between both patterns induced by a variation of the field in agreement with recent experiments.

ACKNOWLEDGMENTS

The authors thank Dr. J. Legrand and V. Germain for fruitful discussions.

APPENDIX

Let $\overline{\mathbf{M}}(\mathbf{r})$ be the x-averaged magnetization

$$\overline{\mathbf{M}}(\mathbf{r}) = 1/L \int_{-L/2}^{L/2} \mathbf{M}(\mathbf{r}) dx. \tag{A1}$$

Due to the symmetry of the studied patterns, the y and z elements of the x-averaged magnetization are zero. It follows immediately that we can restrict ourselves to the calculation of the x element of $\mathbf{H}_d$ which will give M_x from $M_x = \chi(H_0 + H_{d,x})$. $\mathbf{M}$ is replaced by $\overline{\mathbf{M}}$ in Eq. (5). Employing the independence of $\overline{M}_x$ of x, the integral over x in Eq. (5) can be solved analytically. E.g., in the case of a hexagonal pattern, the field due to a cylinder is calculated from

$$H_{i,x}(\mathbf{r}_i) = -\frac{1}{4\pi} \int_{-r_0}^{r_0} dy \int_{-\sqrt{r_0^2-y^2}}^{\sqrt{r_0^2-y^2}} dz \overline{M}_x(\mathbf{r}) \times \left\{ \frac{L/2 - x_i}{[(L/2-x_i)^2 + (y-y_i)^2 + (z-z_i)^2]^{3/2}} - \frac{-L/2 - x_i}{[(-L/2-x_i)^2 + (y-y_i)^2 + (z-z_i)^2]^{3/2}} \right\}. \tag{A2}$$

The computing time for the demagnetization field was drastically reduced using the symmetry properties of the studied patterns. The long-range interaction between the magnetic dipoles is a serious problem in the calculation of the demagnetization field in a magnetic pattern, which is supposed to be infinite in the directions y and z perpendicular to the field. In the case of the hexagonal pattern, the problem was solved in the following way. For the sum in Eq. (6), a spherical cutoff is applied setting $H_{i,x}(\mathbf{r} - \mathbf{r}_i)$ to zero for $r_i > r_c$, where r_c is the cutoff radius. At very large separations from the central cylinder ($r_i \gg r_0$) the difference $(\mathbf{r} - \mathbf{r}_i)$ in Eq. (5) can be replaced by $(\mathbf{r}_i)$. For the x element of $\mathbf{H}_i$, Eq. (5) reduces to

$$H_{i,x}^{lr}(\mathbf{r}_i) = \frac{\pi r_0^2 L \langle M_x \rangle}{4\pi r_i^3} \left\{ -1 + \frac{3x_i^2}{r_i^2} \right\}, \tag{A3}$$

where $\langle M_x \rangle$ is the x element of the volume-averaged magnetization.

Then, a long-range correction for $H_{d,x}$ can be evaluated by integrating $H_{i,x}^{lr}(\mathbf{r}_i)$ due to all the cylinders beyond the cutoff r_c,

$$H_{d,x}^{lr}(\mathbf{r}) = \frac{2\pi\phi}{\pi r_0^2} \int_{r_c}^{\infty} ds s H_{i,x}^{lr}(\mathbf{s}, x) = \frac{L\phi \langle M_x \rangle}{2} \left\{ -\frac{1}{(r_c^2 + x^2)^{1/2}} + \frac{x^2}{(r_c^2 + x^2)^{3/2}} \right\}, \tag{A4}$$

where $\mathbf{s}$ is a vector in the yz plane. In our calculations we took care that the cutoff, beyond which the long-range correction is applied, was sufficiently large to give accurate results. The Ewald summation which is used in other papers [10] is an alternative way to take the long-range interactions into account. It is expected to give the same results.

Particular attention was paid to the computation of $H_{d,x}(\mathbf{r})$ at the bottom and the top of the cylinder, because the integrand in Eq. (A2) has an integrable singularity if $x_i = L/2$ or $x_i = -L/2$.

The derivation of the relationship for the demagnetization field in a striped pattern is very similar to the hexagonal case discussed above.

[1] R. E. Rosensweig, *Ferrohydrodynamics* (Dover Publications, Mineola, 1997).

[2] L. T. Romanikew, M. M. G. Slusarczyk, and D. A. Thompson, IEEE Trans. Magn. **11**, 25 (1975).

[3] A. Cebers and M. M. Maiorov, Magnetohydrodynamics (N.Y.) **16**, 21 (1980).

[4] R. E. Rosensweig, M. Zahn, and R. Shumovich, J. Magn. Magn. Mater. **39**, 127 (1983).

[5] F. Elias, C. Flament, J.-C. Bacri, and S. Neveu, J. Phys. I **7**, 711 (1997).

[6] J.-C. Bacri, R. Perzynski, and D. Salin, Endeavour **12**, 76 (1988).

[7] C.-Y. Hong, I. J. Jang, H. E. Horng, C. J. Hsu, Y. D. Yao, and H. C. Yang, J. Appl. Phys. **81**, 4275 (1997).

[8] C.-Y. Hong, C.-H. Lin, C.-H. Chen, Y. P. Chiu, S. Y. Yang, H. E. Horng, and H. C. Yang, J. Magn. Magn. Mater. **226**, 1881 (2001).

[9] J. Legrand, A. T. N'Go, C. Petit, and M. P. Pileni, Adv. Mater. **18**, 53 (2001).

[10] J. A. Cape and G. W. Lehman, J. Appl. Phys. **42**, 5732 (1971).

[11] A. J. Dickstein, S. Erramilli, R. E. Goldstein, D. P. Jackson, and S. A. Langer, Science **261**, 1012 (1993).

[12] M. Seul and D. Andelman, Science **267**, 476 (1995).

[13] A. T. Dorsey and R. E. Goldstein, Phys. Rev. B **7**, 3058

(1998).
[14] F. M. Ytreberg and S. R. McKay, Phys. Rev. E **61**, 4107 (2000).
[15] A. Gailitis, J. Fluid Mech. **82**, 401 (1977).
[16] R. Friedrichs and A. Engel, Phys. Rev. E **64**, 021406 (2001).
[17] J. Richardi, D. Ingert, and M. P. Pileni, J. Phys. Chem. B **106**, 1521 (2002).
[18] D. Lacoste and T. C. Lubensky, Phys. Rev. E **64**, 041506 (2001).
[19] M. Ivey, J. Liu, Y. Zhu, and S. Cutillas, Phys. Rev. E **63**, 011403 (2001).
[20] I. Drikis, J.-C. Bacri, and A. Cebers, Magnetohydrodynamics (N.Y.) **35**, 203 (1999).
[21] J. D. Jackson, *Classical Electrodynamics*, 3rd ed. (Wiley, New York, 1998).
[22] W. H. Press, B. P. Flannery, S. A. Teukolsky, and W. T. Vetterling, *Numerical Recipes: The Art of Scientific Computing* (Cambridge University Press, Cambridge, 1986).
[23] S. A. Langer, R. E. Goldstein, and D. P. Jackson, Phys. Rev. A **46**, 4894 (1992).
[24] D. P. Jackson, R. E. Goldstein, and A. O. Cebers, Phys. Rev. E **50**, 298 (1994).
[25] A. Cebers and I. Drikis, Magnetohydrodynamics (N.Y.) **32**, 11 (1996).
[26] C. Petit, J. Legrand, V. Russier, and M. P. Pileni, J. Appl. Phys. **91**, 1502 (2002).
[27] J. Richardi and M. P. Pileni (unpublished).
[28] T. C. Halsey and W. Torr, Phys. Rev. Lett. **65**, 2820 (1990).
[29] J. Liu, E. M. Lawrence, A. Wu, M. L. Ivey, G. A. Flores, K. Javier, J. Bibette, and J. Richard, Phys. Rev. Lett. **74**, 2828 (1995).
[30] C. Flament, S. Lacis, J.-C. Bacri, A. Cebers, S. Neveu, and R. Perzynski, Phys. Rev. E **53**, 4801 (1996).
[31] H. Wang, Y. Zhu, C. Boyd, W. Luo, A. Cebers, and R. E. Rosensweig, Phys. Rev. Lett. **72**, 1929 (1994).
[32] K.-O. Ng and D. Vanderbilt, Phys. Rev. B **52**, 2177 (1995).